Biochemical and Biophysical Research Communications 438 (2013) 703–708

Contents lists available at ScienceDirect

Biochemical and Biophysical Research Communications

journal homepage: www.elsevier.com/locate/ybbrc

Design, synthesis and evaluation of a potent substrate analog inhibitor identified by scanning Ala/Phe mutagenesis, mimicking substrate co-evolution, against multidrug-resistant HIV-1 protease

Ravikiran S. Yedidi [a,1], Joseck M. Muhuhi [b,2], Zhigang Liu [a,3], Krisztina Z. Bencze [c], Kyriacos Koupparis [a,b], Carrie E. O'Connor [a], Iulia A. Kovari [a], Mark R. Spaller [b,4], Ladislau C. Kovari [a,*]

[a] Department of Biochemistry and Molecular Biology, School of Medicine, Wayne State University, Detroit, MI 48201, USA
[b] Department of Chemistry, Wayne State University, Detroit, MI 48202, USA
[c] Department of Chemistry, Fort Hays State University, Hays, KS 67601 USA

ARTICLE INFO

Article history:
Received 21 July 2013
Available online 3 August 2013

Keywords:
HIV/AIDS
HIV-1 protease
Protease inhibitors
Multidrug-resistance
CA/p2-analogs
Chemical mutagenesis

ABSTRACT

Multidrug-resistant (MDR) clinical isolate-769, human immunodeficiency virus type-1 (HIV-1) protease (PDB ID: 1TW7), was shown to exhibit wide-open flaps and an expanded active site cavity, causing loss of contacts with protease inhibitors. In the current study, the expanded active site cavity of MDR769 HIV-1 protease was screened with a series of peptide-inhibitors that were designed to mimic the natural substrate cleavage site, capsid/p2. Scanning Ala/Phe chemical mutagenesis approach was incorporated into the design of the peptide series to mimic the substrate co-evolution. Among the peptides synthesized and evaluated, a lead peptide (**6a**) with potent activity (IC_{50}: 4.4 nM) was identified against the MDR769 HIV-1 protease. Isothermal titration calorimetry data showed favorable binding profile for **6a**against both wild type and MDR769 HIV-1 protease variants. Nuclear magnetic resonance spectrum of ^{15}N-labeled MDR769 HIV-1 protease in complex with **6a** showed some major perturbations in chemical shift, supporting the peptide induced conformational changes in protease. Modeling analysis revealed multiple contacts between **6a** and MDR769 HIV-1 protease. The lead peptide-inhibitor, **6a**, with high potency and good binding profile can be used as the basis for developing potent small molecule inhibitors against MDR variants of HIV.

1. Introduction

Acquired immunodeficiency syndrome (AIDS), caused by the human immunodeficiency virus type-1 (HIV-1) infection, claims millions of lives each year (http://www.unaids.org). Currently there are six different classes of FDA-approved drugs available for the treatment of HIV-1 infection, among which, protease inhibitors (PI) have been very successful [1]. HIV-1 protease is a homodimeric aspartyl protease [2] with two catalytic aspartic acid residues, Asp25 and Asp125. Due to the critical requirement of the protease in the life cycle of HIV-1, inhibition of HIV-1 protease for therapeutic intervention, has been evaluated using different strategies [3] – conventional competitive substrate mimics [4], protease dimerization inhibitors [5], allosteric inhibitors [6] and irreversible inhibitors [7] – of which, the conventional approach has been clinically the most successful to date. In fact, all the FDA approved PIs that are currently in clinical use were designed using the conventional approach and incorporate a unique hydroxyl group that mimics the tetrahedral reaction intermediate formed during substrate hydrolysis, resulting in enhanced affinity [8].

Rapid [9] and error-prone replication of HIV-1 incorporates multiple mutations [10] in the viral proteins including the protease. Drug-resistant mutations that are selected under the clinical pressure make the virus, replication-competent in the presence of PIs due to loss of binding affinity of the PI and compensatory

Abbreviations: PI, protease inhibitors; FDA, food and drug administration; CA/p2, Capsid/short peptide; HSQC, heteronuclear single quantum coherence; FRET, fluorescence resonance energy transfer.

* Corresponding author. Address: Department of Biochemistry and Molecular Biology, School of Medicine, Wayne State University, 540 E. Canfield Avenue, Detroit, MI 48201, USA. Fax: +1 313 577 2765.
E-mail address: kovari@med.wayne.edu (L.C. Kovari).
[1] Present address: Experimental Retrovirology Section, HIV and AIDS Malignancy Branch, National Cancer Institute, National Institutes of Health, Bethesda, MD 20892, USA.
[2] Present address: Engineering and Process Sciences, Building 1710, The Dow Chemical Company, Midland, MI 48674, USA.
[3] Present address: Division of Internal Medicine, Harbor Hospital, Baltimore, MD 21225, USA.
[4] Present address: Department of Pharmacology, Geisel School of Medicine at Dartmouth, Lebanon, NH 03756, USA.

0006-291X/$ - see front matter © 2013 Elsevier Inc. All rights reserved.
http://dx.doi.org/10.1016/j.bbrc.2013.07.117

mutations in the substrate that restore substrate binding affinity to the mutant/drug-resistant protease (substrate co-evolution) [11]. Accumulation of mutations in the protease leads to loss of induced-fit against both substrate and PIs but the substrate co-evolution restores the lost induced-fit for the substrate against protease helping the viral replication to continue in the presence of PIs. Crystal structures of multidrug-resistant (MDR) clinical isolate-769 [12] human immunodeficiency type-1 (HIV-1) protease variants show an expanded active site cavity with wide-open conformation of flaps [13,14]. Due to the expanded active site cavity, PIs show loss of contacts [15,16] resulting in loss of potency. In order to restore the potency of PIs, one should understand the organization of the binding pockets by scanning and probing the expanded active site.

In the current study, a series of natural substrate cleavage site, capsid/p2 (CA/p2) (Fig. 1) analog peptide-inhibitors was designed and synthesized using a scanning Ala/Phe chemical mutagenesis approach. The rationale for this approach was to mimic the substrate co-evolution that would yield a lead peptide-inhibitor with best fit (enhanced binding and inhibitory profiles) against the MDR769 HIV-1 protease variants that show expanded active site cavity. Enzyme inhibition assays were performed to identify lead peptide-inhibitor (**6a**). Isothermal Titration Calorimetry (ITC), Nuclear Magnetic Resonance (NMR) spectroscopy and molecular modeling were performed to understand the binding of **6a** to the MDR769 HIV-1 protease.

2. Materials and methods

2.1. Synthesis of peptide-inhibitors

Details of the synthetic procedures including synthetic schemes are given in the supplementary information associated with this article.

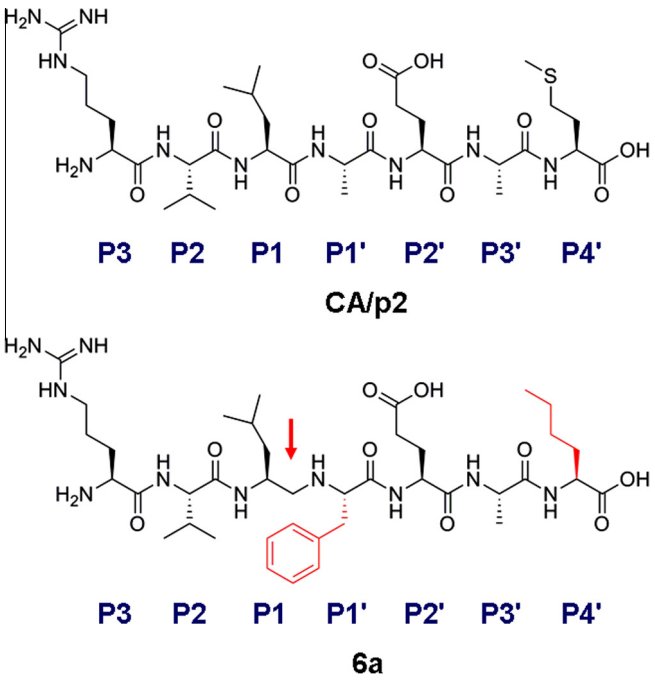

Fig. 1. Structures of CA/p2 and lead peptide-inhibitor, **6a**. Top panel shows the structure of CA/p2 substrate cleavage site peptide spanning from P3 to P4′. Bottom panel shows the lead peptide-inhibitor, **6a**, with modifications highlighted in red at P1′ and P4′. The labile peptide bond between P1 and P1′ in CA/p2 is replaced with a reduced peptide bond (–CH_2–NH–) in **6a** (indicated by the red arrow). (For interpretation of the references to color in this figure legend, the reader is referred to the web version of this article.)

2.2. Enzyme inhibition assay

Fluorescence resonance energy transfer (FRET)-based enzyme inhibition assays were performed as described previously [16] using fluorogenic HIV-1 substrate (purchased from Molecular Probes – California, USA). The wild type (NL4-3) HIV-1 protease was purchased from Bachem at a concentration of 0.3 mg/ml. Active MDR769 HIV-1 protease was expressed and purified as described previously [17]. The final purified active MDR769 HIV-1 protease was at a concentration of 0.5 mg/ml. The final IC_{50} values reported here represent the average of three independent experiments.

2.3. Expression and purification of ^{15}N-labeled MDR769 HIV-1 protease

Expression and purification of ^{15}N-labeled MDR769 HIV-1 protease was performed using a modified protocol described previously [17]. Briefly, the BL21-DE3 (pLysE) *Escherichia coli* cells were transformed with pRSET-B plasmid harboring the MDR769 (D25N + A82T) HIV-1 protease gene cloned in frame with an Isopropyl β-D-1-thiogalactopyranoside (IPTG) inducible T7 promoter. The D25N mutation was to prevent protease auto-proteolysis and the A82T mutation was to perform a direct comparison between the NMR and crystal structure in future. Crystallization trials of MDR769 (D25N + A82T) in complex with **6a** are currently in progress. A82T mutation was found to enhance the crystallizability of MDR769 HIV-1 protease (example PDB IDs: 3R0W, 3R0Y, 4EYR). The transformed *E. coli* cells were grown in 20 ml of Luria Bertani (LB) medium to OD_{600} of 1.0. The cells were harvested as a pellet and the pellet was resuspended in 500 ml of 1X M9, minimal medium. Cells were cultured in the M9 medium until OD_{600} of 0.8. The cells were harvested by centrifugation and the cell pellet was used to inoculate 2 L of ^{15}N-labeled M9 medium containing ^{15}N-NH4Cl. The cells were cultured up to an OD_{600} of 0.4. Protease expression was induced with 1 mM IPTG. Cultures were grown for 6 h. The cells were harvested by centrifugation at 2500 rpm for 30 min. and were lysed using a French press. Inclusion bodies were harvested from the cell extracts and were dissolved in 6 M urea. Denatured protease was purified using ion-exchange chromatography and was refolded by dialysis. Refolded protease was further concentrated using Amicon filters (EMD Millipore - Massachusetts, USA).

2.4. Isothermal Titration Calorimetry

ITC measurements were performed on a VP-ITC microcalorimeter (MicroCal, Inc., Northampton, USA). Samples of MDR769 (D25N + A82T) protease were prepared at concentrations in the range of 20–120 μM. Peptide concentrations were kept constant at either 2 or 3 mM. Temperature was either 25, 30 or 37 °C. After the initial 1 μL injection there were 19 or 29 additional injections of 10 or 15 μL, respectively. Spacing between injections was kept at either 180 or 210 s. The stirring speed of the injector syringe was kept constant at 500 rpm. The protease and the peptides were all in 10 mM sodium acetate buffer at or around pH 7.0. The best result (isotherm shown in Fig. 2) was collected on **6a** peptide at 30 °C with MDR769 (D25N + A82T) HIV-1 protease concentration of 70–118 μM, peptide concentration of 2 mM, 29 injections, and 180 s. time between injections. Similar conditions were used for NL4-3 to obtain the binding isotherm for **6a**. Data analysis was performed using the Origin 5.0 software supplied by MicroCal Inc. The software uses a nonlinear least-square curve-fitting algorithm to calculate the dissociation constant, stoichiometric ratio and change in enthalpy of the reaction. All the final values were

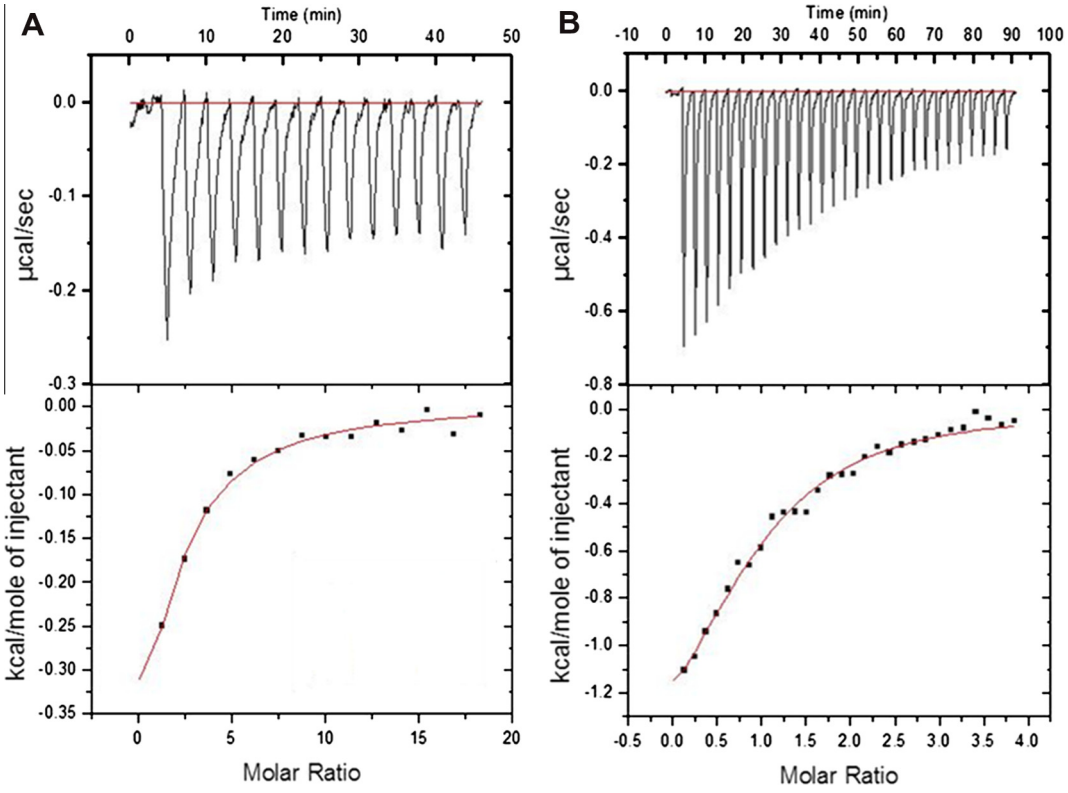

Fig. 2. Isothermal titration calorimetric (ITC) analysis of **6a**. Panels a and b show the ITC evaluation of **6a** against wild type (NL4-3) and MDR769 HIV-1 protease variants, respectively. In each panel, the raw data is shown on the top and the binding isotherm is shown at the bottom. The red line in the raw ITC data indicates base line while the red line in binding isotherm indicates the curve fit to the data points. **6a** shows favorable binding profiles against both NL4-3 and MDR769 HIV-1 protease variants. (For interpretation of the references to color in this figure legend, the reader is referred to the web version of this article.)

Table 1
IC_{50} (nM) values of peptide-inhibitors against wild type (NL43) and MDR769 HIV-1 protease variants.

Compound	Sequence	IC_{50} [a] ± SD[b]	
	P3-P2-P1-r[c] -P1′-P2′-P3′-P4′	Wild type	MDR769
6a	Arg-Val-Leu-r-PHE-Glu-Ala-Nle	2.60 ± 0.4	4.40 ± 0.7
6b	Arg-ALA-Leu-r-Phe-Glu-Ala-Nle	78.20 ± 11.7	74.10 ± 10.4
6c	Arg-PHE-Leu-r-Phe-Glu-Ala-Nle	>1000	770.00 ± 62.9
6d	Arg-Val-ALA-r-Phe-Glu-Ala-Nle	>1000	>1000
6e	Arg-Val-PHE-r-Phe-Glu-Ala-Nle	31.00 ± 14.6	142.00 ± 4.0
6f	Arg-Val-Leu-r-Phe-ALA-Ala-Nle	232.00 ± 30.0	234 ± 3.21
6g	Arg-Val-Leu-r-Phe-PHE-Ala-Nle	>1000	>1000
7a	Phe-Glu-Ala-Nle	>1000	>1000
7b	Arg-Val-Leu	>1000	>1000

[a] IC_{50}-half maximal inhibitory concentration.
[b] SD-standard deviation.
[c] Reduced peptide bond (-r-) to avoid cleavage by protease.

average obtained from two independent experiments. ΔG values were calculated using the equation $\Delta G = \Delta H - T\Delta S$.

2.5. NMR spectroscopy of ^{15}N-labeled MDR769 HIV-1 protease

NMR experiments were performed on a Varian INOVA 600 MHz spectrometer (located at the Eugene Applebaum College of Pharmacy & Health Sciences, Wayne State University, Detroit, MI) equipped with a triple-resonance $^{1}H/^{13}C/^{15}N$ cold probe with z-axis pulsed field gradients. Samples of protease were prepared at 100 µM in 10 mM sodium acetate buffer, pH 5.0 and experiments were run at 22 °C. $^{1}H/^{15}N$-HSQC were collected with a ^{1}H sweep width of 10,000 Hz, 2048 points and 32 transients, and with ^{15}N sweep width of 3000 Hz, and 512 increments. The same sample was re-run with the same parameters after the addition of **6a** at 20-fold excess. Spectra were referenced using an external 4,4-dimethyl-4-silapentane-1-sulfonic acid (DSS) control sample [18]. Data were transformed using NMRPipe [19]. Peak identifications were done partially based on previously published chemical shifts for the wild type protease [20] and labeled using Sparky [21].

2.6. Docking analysis of *6a* against MDR769 HIV-1 protease

All the docking experiments were performed using AutoDock Vina [22] as described previously [16]. Briefly, PDB IDs: 1TW7 (MDR769 HIV-1 protease with wide-open flaps) and 3SO9 (MDR769 HIV-1 protease with closed flaps) were used as receptors, which were prepared before docking, using AutoDock tools [23] (ADT)-GUI (Graphic User Interface). The molecular model for **6a** was also prepared using ADT-GUI prior to the docking. All the molecular graphics in this article were prepared using the open source PyMol (Ver. 0.99rc6) program (http://www.pymol.org).

3. Results

3.1. Design of the peptide-inhibitor library

As shown in Table 1, a series of nine peptides (**6a**–**6g**), including two short peptides (**7a** and **7b**), was designed. The labile peptide bond (–CO–NH–) in peptides **6a-6g** was replaced with a reduced peptide bond [24] (–CH_2–NH–) to avoid cleavage by the protease in the enzyme assays. Peptides **6a-6g** span from P3-Arg to P4′-Nle while the two short peptides, **7a** and **7b** represent

P1′-P2′-P3′-P4′ and P3-P2-P1 groups, respectively from the CA/p2 peptide. The Met residue at P4′ was replaced by isosteric Nle for synthetic convenience. Previously it has been shown that replacement of Ala at P1′ with derivatives of Phe enhanced binding of CA/p2 peptide to HIV-1 protease [25]. Moreover, all the FDA approved PIs that are currently in use consist of at least one phenyl group either at P1 or at P1′. In the current study, all the peptides consist of Phe at P1′ position to enhance the overall binding of the peptide to the MDR769 HIV-1 protease.

3.2. Lead peptide (**6a**) shows >16- to >220-fold higher potency

A highly potent lead peptide, **6a**, (Fig. 1) was identified against the MDR769 HIV-1 protease in the enzyme inhibition assays (Table 1). This is the first report of a highly potent substrate-analog peptide-inhibitor against MDR769 HIV-1 protease. The lead peptide, **6a**, showed >16-fold higher potency than that of **6b** against MDR769 HIV-1 protease (Table 1). Similarly, **6a** showed >30- and >50-fold higher potency over the peptides **6e** and **6f**, respectively. **6a** showed >170- to >220-fold higher potency compared to **6c** and other peptides, respectively, in the series screened against the expanded active site cavity of MDR769 HIV-1 protease (Table 1). The two short peptides (**7a** and **7b**) were evaluated individually and also as a combined mixture. The potency of **7a** and **7b**, either individually or together, was weaker compared to that of **6a**, against MDR769 HIV-1 protease. While **6a** and **6b** showed similar potency against both wild type (NL4-3) and MDR769 HIV-1 protease variants, **6e** showed good potency against NL4-3 than the MDR769. Based on the higher potency, the binding profile of **6a** with MDR769 HIV-1 protease was further evaluated using ITC and NMR spectroscopy.

3.3. **6a** shows favorable binding isotherms against NL4-3 and MDR769 HIV-1 protease variants

ITC analysis showed favorable binding profiles for **6a** against both NL4-3 and MDR769 HIV-1 protease variants. The binding isotherms including raw data for **6a** are shown in Fig. 2. The K_d values for **6a** against NL4-3 and MDR769 were 86 μM and 68 μM, respectively. Analysis of thermodynamic parameters revealed favorable binding affinities (Gibb's free energy, ΔG), for **6a** against both NL4-3 (ΔG: -5.60 ± 0.04 kcal/mol.) and MDR769 (ΔG: -5.82 ± 0.09 kcal/mol.) HIV-1 protease variants. Among the peptide series, **6a** showed the best binding profile against MDR769 HIV-1 protease. In order to further investigate the poor binding profiles of the peptides in the series other than **6a**, an effort to optimize the ITC analysis will need to be performed in the future.

3.4. Peptide-induced perturbations in the ^{15}N-HSQC spectra

In order to confirm the binding of **6a** to MDR769 HIV-1 protease, the ^{15}N-HSQC spectra of ^{15}N-labeled MDR769 HIV-1 protease in the presence and absence of **6a** were obtained and analyzed. Analysis of the ^{15}N-HSQC spectra of MDR769 HIV-1 protease in the presence and absence of lead peptide (**6a**) showed perturbations in the chemical shifts (either ^{1}H or ^{15}N or both). As shown in Figure S1, the overlay of the two spectra exhibits well-distributed peaks confirming the folded form of the protease in both cases. As shown in Fig. 3, perturbations were seen both in and around the active site cavity. Peak splitting, peak shifting (examples shown in Fig. 3) were seen in more than 50% of the peaks, indicating peptide induced conformational changes in the MDR769 HIV-1 protease. The peaks in the overlay of the spectra, as shown in Figure S1, show similar distribution to the peaks of MDR769 HIV-1 protease ^{15}N-HSQC spectrum that was recently published by another group [26]. Based on the analysis of assigned peaks, Thr4, Trp6, Gln7, Ile10, Val11, Thr12, Gly16, Leu19, Lys20, Ala22, Leu23, Thr26, Gly27, Ala28, Asp29, Asp30, Val32, Asn37, Leu38, Trp42, Ile47, Gly48, Gly51, Lys55, Val56, Gln58, Tyr59, Glu65, Ile66, Lys70, Thr74, Val75, Leu76, Val77, Thr82, Asn83, Arg87, Asn88, Thr91, Gln92, Ile93, Gly94 and Cys95 were identified as the residues that showed major perturbations. Residues, Arg8, Gly17, Gln18, Glu34, Val36, Arg57, Asp60, Gln61, Val62, Gly68, His69, Met90 and Leu97 showed minor perturbations. Very small to negligible perturbations were seen for residues Gly2, Ile3, Ile13, Ile15, Leu24, Leu33, Gly40, Arg41, Lys43, Leu46, Phe53, Ile72, Gly73, Thr80, Val84, Asn98 and Phe99. Among the 43 residues that showed perturbations, 15 residues were identified to be from the expanded active site cavity that contribute to the ligand binding. These residues are mapped as red spheres in Fig. 3. Similarly, among the residues that showed negligible perturbations, Leu24, Thr80 and Val84 were identified to be from the expanded active site cavity. In order to further understand the binding-interactions, docking analysis of **6a** was performed.

3.5. Docking models revealed multiple interactions between **6a** and MDR769 HIV-1 protease

Molecular model of **6a** was docked against two docking receptors, PDB IDs: 1TW7 (MDR769 HIV-1 protease with wide-open conformation of the flaps) and 3SO9 (MDR769 HIV-1 protease with closed conformation of the flaps). These docking models of **6a** helped in mapping new binding sites in the expanded active site of the MDR769 HIV-1 protease that may be targeted in designing future potent PIs. As shown in Fig. 4, **6a** shows multiple polar and hydrophobic contacts with MDR769 HIV-1 protease docking receptor – 3SO9. The total number of polar contacts made by **6a** with 1TW7 and 3SO9 were 3 and 7, respectively. Similarly, the total number of hydrophobic contacts made by **6a** with 1TW7 and 3SO9 were 28 and 37, respectively. This indicates enhanced binding profile of **6a** to the protease with closed flap conformation. Additionally, when 3SO9 was used as docking receptor, the binding profile of **6a** was similar to that of substrate (CA/p2) peptide (PDB ID: 1DAZ).

4. Discussion

4.1. **6a** shows favorable inhibition and binding profiles against MDR769 HIV-1 protease

The current study shows that by using the scanning Ala/Phe chemical mutagenesis approach to mimic the natural substrate co-evolution process, one can identify a lead peptide-inhibitor with restored induced-fit against the MDR769 HIV-1 protease with expanded active site cavity and wide-open flaps. Comparative analysis of the potencies of peptide-inhibitors **6a-6g** revealed that replacement of Val (P2), Leu (P1) or Glu (P2′) with Ala (less bulky side chain) resulted in 17-, >227- or 53-fold loss in potency, respectively, against MDR769 HIV-1 protease. Similarly, replacement of Val (P2), Leu (P1) or Glu (P2′) with Phe (bulky side chain) resulted in 175-, 32- or >227-fold loss of potency, respectively, against MDR769 HIV-1 protease. Thus, Val at P2, Leu at P1 and Glu at P2′ positions are critical and required for the potency of **6a** against MDR769 HIV-1 protease. The peptide-inhibitors, **6f** and **6g** reconfirmed the importance of Glu at P2′ position as reported previously [27]. Further, addition of a hydroxyl group between P1 and P1′ residues of **6a** might increase its potency by enhancing the binding affinity. Considering the higher potency of **6a** (Table 1), in combination with favorable binding profile (ΔG: -5.82 ± 0.09 kcal/mol.) against MDR769 HIV-1 protease, which exhibits expanded active

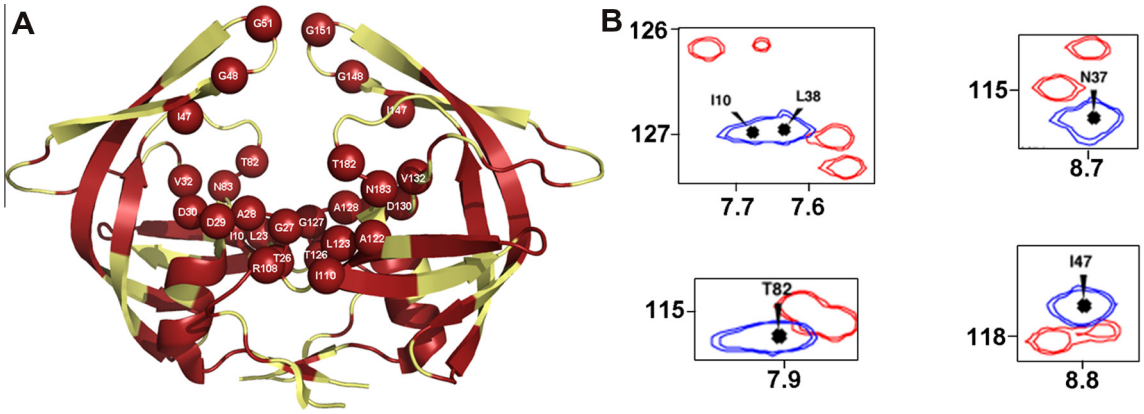

Fig. 3. Mapping the residues from the perturbations in NMR ^{15}N-HSQC spectra. Panel a shows MDR769 HIV-1 protease dimer (yellow color) with residues labeled from 1–99 and 101–199 for monomers 1 and 2, respectively. Domains that show perturbations upon addition of **6a** are shown in red. Active site residues that showed major perturbations and are critical in ligand binding are highlighted as red spheres. Panel b shows selected peaks that show perturbations (peak shifting and peak splitting) upon addition of **6a**. Blue and red peaks indicate before and after the addition of **6a**, respectively, to the protease. The horizontal and vertical axes represent ^{1}H (ppm) and ^{15}N (ppm), respectively. (For interpretation of the references to color in this figure legend, the reader is referred to the web version of this article.)

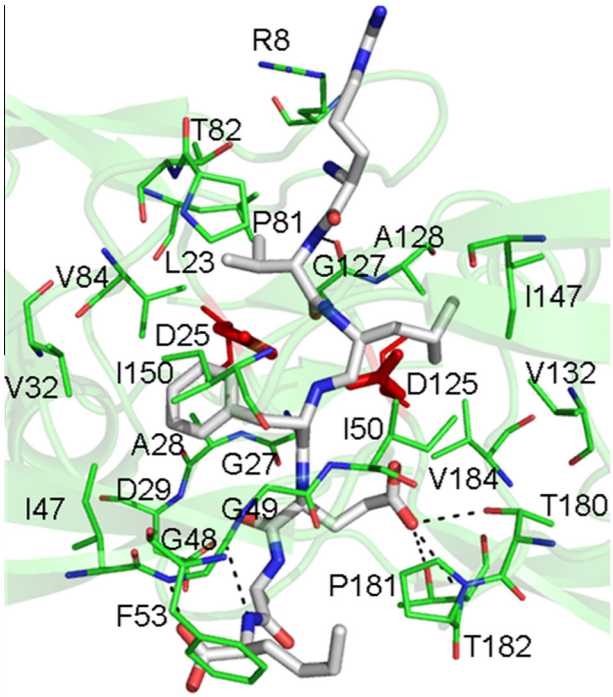

Fig. 4. Docking model of **6a** showing contacts. Docking model of **6a** is shown as white stick model in the active site of MDR769 HIV-1 protease with closed flaps (PDB ID: 3SO9). Protease residues involved in polar and hydrophobic contacts with **6a** are highlighted as green stick models. Polar contacts are shown as black dashed-lines. The catalytic Asp25 and Asp125 are shown as red stick models. Protease residues are labeled 1–99 and 101–199 for monomers 1 and 2, respectively. (For interpretation of the references to color in this figure legend, the reader is referred to the web version of this article.)

site cavity and wide-open flaps, **6a** can be used as a lead peptide to design future potent small molecule PIs.

*4.2. Binding of **6a** to MDR769 HIV-1 protease may induce partial if not complete flap closure*

The perturbations observed in the ^{15}N-HSQC spectra of ^{15}N-labeled MDR769 HIV-1 protease in the presence and absence of **6a** confirmed its binding in the expanded active site cavity of MDR769 HIV-1 protease. Among the residues with major perturbations, 17 were identified from flap region that contribute to the protease flap open/close mechanism and 15 were from the expanded active site cavity suggesting major ligand-induced conformational changes in the wide-open flaps and may imply that **6a** induces complete flap closure in MDR769 HIV-1 protease variants yielding nanomolar potency. Docking analysis of **6a** against MDR769 HIV-1 protease receptor revealed multiple polar and hydrophobic contacts with 25 residues among which, 14 residues showed major perturbations in the NMR spectrum confirming the ligand binding. Residues Thr80, Pro81 and Val84 showed contacts in the docking models but did not show significant perturbations suggesting that these residues may be involved in tighter binding with **6a** without major conformational changes. Of note, **6a** showed a conserved polar contact with Thr80 in both receptors, 1TW7 and 3SO9. Thr80 is an amino acid that rarely undergoes mutation in the HIV-1 protease gene and the conserved polar contact with Thr80 might in part explain the higher potency of **6a** against MDR769 HIV-1 protease.

*4.3. Closed flap docking receptor shows enhanced contacts with **6a***

MDR769 HIV-1 protease variants (PDB IDs: 1TW7, 3OQ7, 3OQA, 3OQD and 3PJ6) are known to show wide-open conformation of the flaps due to accumulation of multiple mutations. In order to understand the binding profile of **6a** in the active site cavity of such wide-open flaps containing receptor, 1TW7 was used as receptor. This method (using 1TW7 as docking receptor) showed the adaptation of peptide conformation in the expanded active site cavity. On the other hand, the docking method using 3SO9 as receptor depicts the peptide induced complete flap closure of the MDR protease. Due to closed flap conformation of the receptor (3SO9), **6a** showed enhanced polar contacts (increased from a total of 3 polar contacts to a total of 7 polar contacts) as well as hydrophobic contacts (increased from a total of 28 hydrophobic contacts to a total of 37 hydrophobic contacts) compared to that of 1TW7. Enhanced binding profile with more contacts in the active site cavity of receptor 3SO9 suggests that **6a** may induce complete flap closure in MDR769 HIV-1 protease variants yielding nanomolar potency.

Taken together, the current structure–activity studies confirmed the hypothesis that the scanning Ala/Phe chemical mutagenesis approach mimicking the substrate co-evolution would yield a better induced-fit. Considering the higher potency, **6a** can be used as a lead peptide to design future potent small molecule PIs against MDR variants of HIV-1 protease that exhibit expanded

active site cavity and wide-open flaps. However, **6a** may not be used as a therapeutic as is, due to its peptidic nature, which may cause poor cell penetration properties.

Acknowledgment

We thank the National Institutes of Health for funding to LCK (grant#AI65294) and IMSD/MBRS fellowship to JMM (NIH-R25GM058905).

Appendix A. Supplementary data

Supplementary data associated with this article can be found, in the online version, at http://dx.doi.org/10.1016/j.bbrc.2013.07.117.

References

[1] A.K. Ghosh, B.D. Chapsal, I.T. Weber, H. Mitsuya, Design of HIV protease inhibitors targeting protein backbone: an effective strategy for combating drug resistance, Acc. Chem. Res. 41 (2008) 78–86.
[2] T.D. Meek, B.D. Dayton, B.W. Metcalf, et al., Human immunodeficiency virus 1 protease expressed in *Escherichia coli* behaves as a dimeric aspartic protease, Proc. Natl. Acad. Sci. USA 86 (1989) 1841–1845.
[3] F. Lebon, M. Ledecq, Approaches to the design of effective HIV-1 protease inhibitors, Curr. Med. Chem. 7 (2000) 455–477.
[4] C. Debouck, The HIV-1 protease as a therapeutic target for AIDS, AIDS Res. Hum. Retroviruses 8 (1992) 153–164.
[5] M.D. Shultz, Y.W. Ham, S.G. Lee, et al., Small-molecule dimerization inhibitors of wild-type and mutant HIV protease: a focused library approach, J. Am. Chem. Soc. 126 (2004) 9886–9887.
[6] A.L. Perryman, Q. Zhang, H.H. Soutter, et al., Fragment-based screen against HIV protease, Chem. Biol. Drug Des. 75 (2010) 257–268.
[7] J.J. DeVoss, Z. Sui, D.L. DeCamp, et al., Haloperidol-based irreversible inhibitors of the HIV-1 and HIV-2 proteases, J. Med. Chem. 37 (1994) 665–673.
[8] T. Mimoto, J. Imai, S. Tanaka, et al., Rational design and synthesis of a novel class of active site-targeted HIV protease inhibitors containing a hydroxymethylcarbonyl isostere. Use of phenylnorstatine or allophynylnorstatine as a transition-state mimic, Chem. Pharm. Bull. (Tokyo) 39 (1991) 2465–2467.
[9] A.S. Perelson, A.U. Newmann, M. Markowitz, et al., HIV-1 dynamics in vivo: virion clearance rate, infected cell life-span, and viral generation time, Science 271 (1996) 1582–1586.
[10] B.D. Preston, J.P. Dougherty, Mechanisms of retroviral mutation, Trends Microbiol. 4 (1996) 16–21.
[11] L. Doyon, G. Croteau, D. Thibeault, et al., Second locus involved in human immunodeficiency virus type 1 resistance to protease inhibitors, J Virol. 70 (1996) 3763–3769.
[12] S. Palmer, R.W. Shafer, T.C. Merigan, Highly drug-resistant HIV-1 clinical isolates are cross-resistant to many antiretroviral compounds in current clinical development, AIDS 13 (1999) 661–667.
[13] P. Martin, J.F. Vickrey, G. Proteasa, et al., "Wide-open" 1.3 Å structure of a multidrug-resistant HIV-1 protease as a drug target, Structure 13 (2005) 1887–1895.
[14] R.S. Yedidi, G. Proteasa, J.L. Martinez, et al., Contribution of the 80's loop of HIV-1 protease to the multidrug-resistance mechanism: crystallographic study of MDR769 HIV-1 protease variants, Acta Crystallogr. D Biol. Crystallogr. 67 (2011) 524–532.
[15] B.C. Logsdon, J.F. Vickrey, P. Martin, et al., Crystal structures of a multidrug-resistant human immunodeficiency virus type 1 protease reveal an expanded active-site cavity, J. Virol. 78 (2004) 3123–3132.
[16] R.S. Yedidi, Z. Liu, Y. Wang, et al., Crystal structures of multidrug-resistant HIV-1 protease in complex with two potent anti-malarial compounds, Biochem. Biophys. Res. Commun. 421 (2012) 413–417.
[17] J.F. Vickrey, B.C. Logsdon, G. Proteasa, et al., HIV-1 protease variants from 100-fold drug resistant clinical isolates: expression, purification, and crystallization, Protein. Expr. Purif. 28 (2003) 165–172.
[18] D.S. Wishart, C.G. Bigam, J. Yao, et al., ^{1}H, ^{13}C and ^{15}N chemical shift referencing in biomolecular NMR, J. Biomol. NMR 6 (1995) 135–140.
[19] F. Delaglio, S. Grzesiek, G.W. Vuister, et al., NMR Pipe: a multidimensional spectral processing system based on UNIX pipes, J. Biomol. NMR 6 (1995) 277–293.
[20] E. Katoh, J.M. Louis, T. Yamazaki, et al., A solution NMR study of the binding kinetics and the internal dynamics of an HIV-1 protease–substrate complex, Protein Sci. 12 (2003) 1376–1385.
[21] T.D. Goddard, D.G. Kneller, SPARKY 3.0, University of California, San Francisco, 2001.
[22] O. Trott, A.J. Olson, AutoDock Vina: improving the speed and accuracy of docking with a new scoring function, efficient optimization and multithreading, J. Comput. Chem. 31 (2010) 455–461.
[23] M.F. Sanner, Python: a programming language for software integration and development, J. Mol. Graph. Model. 17 (1999) 57–61.
[24] J. Urban, J. Konvalinka, J. Stehlikova, et al., Reduced-bond tight-binding inhibitors of HIV-1 protease. Fine tuning of the enzyme subsite specificity, FEBS Lett. 298 (1992) 9–13.
[25] A.D. Richards, L.H. Phylip, W.G. Farmerie, et al., Sensitive, soluble chromogenic substrates for HIV-1 proteinase, J. Biol. Chem. 265 (1990) 7733–7736.
[26] X. Huang, I.M.S deVera, A.M. Veloro, et al., Backbone ^{1}H, ^{13}C, and ^{15}N chemical shift assignments for HIV-1 protease subtypes and multi-drug resistant variant MDR 769, Biomol. NMR Assign (2012) 1–4.
[27] I.T. Weber, J. Wu, J. Adomat, et al., Crystallographic Analysis of Human Immunodeficiency Virus 1 Protease with an analog of the conserved CA-p2 substrate—interactions with frequently occurring glutamic acid residue at P2′ position of substrates, Eur. J. Biochem. 249 (1997) 523–530.